Design and Synthesis Methodology for UHF-RFID Tags Based on the T-match Network

Gerard Zamora, Simone Zuffanelli, Ferran Paredes, Ferran Martín, *Fellow, IEEE,* and Jordi Bonache, *Member, IEEE*

Abstract—**A new systematic methodology for the design of T-match based UHF-RFID tags is proposed. The great majority of commercial UHF-RFID tags are based on dipole antennas using a modification of a T-match network. The literature contains examples of models that describe the T-match, but they are not sufficiently accurate to synthesize the tag geometry. Using the proposed methodology, a global band UHF-RFID tag based on a folded dipole antenna and matched to the RFID integrated circuit by means of a T-match network is designed and fabricated. Very good agreement between the measured and simulated read range is achieved within the entire UHF-RFID band, which reveals that the proposed method is amenable for accurate analysis and synthesis of T-match based UHF-RFID tags.**

***Index Terms*— Radio frequency identification (RFID), T-match network, tags, antennas.**

I. Introduction

RADIO frequency identification (RFID) is a rapidly developing technology that provides wireless identification and tracking capability. Particularly, passive ultra-high frequency (UHF) RFID systems are very attractive in comparison with passive RFID regulated systems using low frequency (LF) and high frequency (HF) bands, since they can provide superior read range, fast reading and enhanced information storage ability [1]. The regulated UHF-RFID bands vary in the different world regions, including frequencies between 840 MHz and 960 MHz. More specifically, RFID is operated at 840-845 MHz in China, at 866-869 MHz in Europe, at 902-928 MHz in USA and at 950-956 MHz in Japan. Therefore, the design of inlay tags able to cover the whole regulated UHF bands (i.e., global band tags) becomes an important challenge.

A passive UHF-RFID system consists of a reader and a tag, which includes an antenna matched to an application specific integrated circuit (ASIC) chip. Generally, the chip impedance is capacitive, thereby requiring the antenna impedance to be inductive in order to obtain a proper impedance matching (conjugate matching). Several techniques for achieving conjugate matching can be found in the literature [2], [3].

This work was supported by Spain MICIIN under projects CONSOLIDER CSD2008-00066 and METATRANSFER TEC2010-17512, and by AGAUR (Generalitat de Catalunya) through the project 2009SGR-421.

The authors are with GEMMA/CIMITEC (Departament d'Enginyeria Electrònica), Universitat Autònoma de Barcelona. 08193 BELLATERRA (Barcelona). Spain. E-mail: Gerard.Zamora@uab.cat.

.

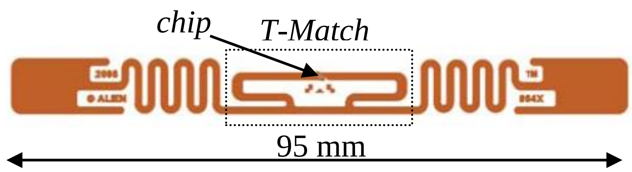

Fig. 1. Example of a UHF-RFID commercial tag based on the T-match network (*Alien ALN-9640*).

However, most commercial UHF-RFID tags are based on dipole antennas using some variant of a T- match network [4]-[6]. The T-match connection was first proposed by Uda [7], and more recently explained in [8] as an effective shunt-matching technique. Although it was initially analyzed as a general form of a cylindrical folded dipole, the Uda model has been applied to design planar structures [9]-[11] and even RFID tags [2],[4],[5]. However, many approximations are assumed when planar conductor shapes are considered [8]. Moreover, by this means, only a special case of the T-match structure can be used to design RFID tags, the embedded T-match, that is constructed by embedding the T-match structure into the antenna [6]. This is the main drawback since most commercially available T-match based tags have more complex geometries which cannot be analyzed by means of this planar model. An example of these tags is depicted in Fig. 1, where the T-match network has a loop shape and is located at the center of the tag. In order to overcome this problem, some efforts to deviate from Uda classic analysis and focus on a circuit-based approach have been made [5],[12],[13]. In these works, equivalent-circuit models of a dipole antenna (only valid over a relatively small frequency range near resonance) matched to the chip by means of a T-match have been developed. Nevertheless, the synthesis process of the tags from the obtained circuits is not fully explained.

In this paper, a new and very simple systematic method for the design and synthesis of global band UHF-RFID tags based on the T-match network is presented. Such method is based on a new equivalent-circuit model approach. Moreover, the frequency limits related to the validity of the presented approach are studied, and the dependence of the achieved tag bandwidth with the antenna impedance is also discussed. To illustrate the potential of the approach, an RFID tag is designed and synthetized through this method and the read range of the fabricated prototype is measured.

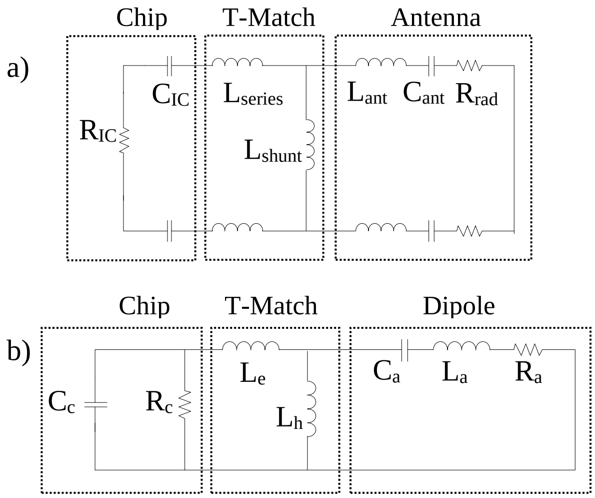

Fig. 2. (a) Balanced equivalent-circuit model of a T-match based UHF-RFID tag from [13], and (b) unbalanced equivalent-circuit model reported in [5].

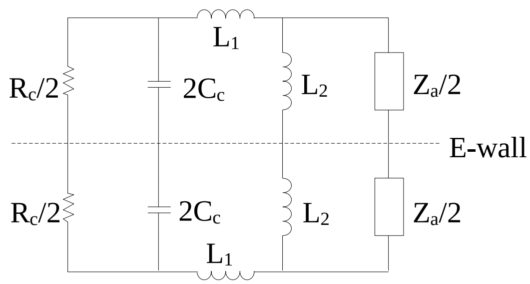

Fig. 3. Equivalent-circuit model of a T-match based UHF-RFID tag using the electric wall concept.

II. Equivalent Circuit Model of T-Match based Tags: New Approach and Requirements

The T-match structure, shown in Fig. 1, is the most common matching network used for the efficient matching of UHF-RFID tags. Since this network is electrically small at the UHF-RFID regulated bands (840-960 MHz), a lumped-element equivalent-circuit model can be considered. Moreover, it is well known that the input impedance of a UHF-RFID chip can be modeled by a parallel combination of a resistance R_c and a capacitance C_c [14], [15]. Thus, a circuit model for the T-match structure cascaded to a commercial RFID chip can be obtained, which is of special interest for tag design. Some efforts to obtain an equivalent-circuit model for the T-match network cascaded to the chip can be found in the literature. In [13], the circuit diagram shown in Fig. 2(a) is proposed, whereas in [5] this balanced circuit is reduced to an unbalanced version, depicted in Fig. 2(b). Although this circuit is complete and reasonably accurate, the authors in [5] transformed the matching circuit from a series-shunt connection of L_e and L_h into a shunt-series connection with a scaled load impedance. This allows reformulating the tag antenna and matching circuit problem into a classical two stage bandpass filter. The main drawback of such approach is the difficulty to synthesize the tag antenna and matching circuit, once the circuit model is tuned. Moreover, the authors do not give details about how to synthesize the presented tags from the circuit model.

In this work, due to the symmetry of T-match based tags and the differential mode excitation, forced by the chip, the

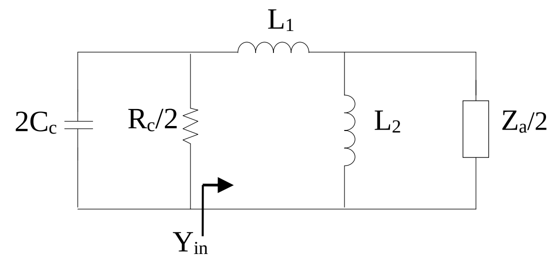

Fig. 4. Equivalent-circuit model of one half of a T-match based UHF tag.

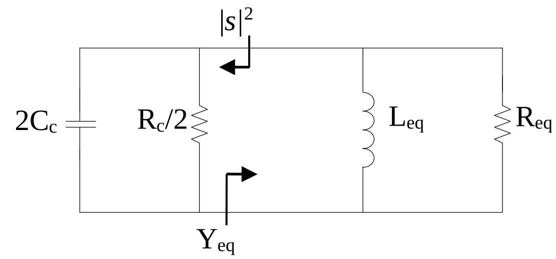

Fig. 5. Equivalent-circuit model of the circuit of Fig. 4.

electric wall concept has been used in order to obtain an equivalent-circuit model (see Fig. 3). The required values of the circuit elements can be obtained by considering only one-half of the network (see Fig. 4). In this equivalent-circuit, the antenna impedance, $Z_a = R_a + j\chi_a$, is modeling any general impedance. It can be observed that the circuit cascaded between the chip and the antenna is an inductive transformer [16]. Thus, the circuit of Fig. 4 can be modeled by the circuit depicted in Fig. 5. To demonstrate this, the admittances $Y_{in} = G_{in} + jB_{in}$ and $Y_{eq} = G_{eq} + jB_{eq}$, given by

$$G_{in} = \frac{2L_2^2 R_a}{|Z_a|^2 (L_1+L_2)^2 + 4\omega^2 L_1^2 L_2^2 + 4\omega\chi_a L_1 L_2 (L_1+L_2)} \quad (1)$$

$$B_{in} = \frac{-\left[|Z_a|^2 (L_1+L_2) + 4\omega^2 L_2^2 L_1 + 2\omega\chi_a \left(L_2^2 + 2L_1 L_2\right)\right]}{\omega\left[|Z_a|^2 (L_1+L_2)^2 + 4\omega^2 L_1^2 L_2^2 + 4\omega\chi_a L_1 L_2 (L_1+L_2)\right]} \quad (2)$$

$$Y_{eq} = G_{eq} + jB_{eq} = \frac{1}{R_{eq}} - j\frac{1}{\omega L_{eq}} \quad (3)$$

are forced to be equal. Comparing the real part one obtains:

$$R_{eq} = \frac{|Z_a|^2 (L_1+L_2)^2 + 4\omega^2 L_1^2 L_2^2 + 4\omega\chi_a L_1 L_2 (L_1+L_2)}{2L_2^2 R_a} \quad (4)$$

If $(R_a^2+\chi_a^2)(L_1+L_2)^2 >> |4\omega^2 L_1^2 L_2^2 + 4\omega\chi_a L_1 L_2 (L_1+L_2)|$ is satisfied, then expression (4) can be approximated by

$$R_{eq} = \left(1+\frac{L_1}{L_2}\right)^2 \left(\frac{R_a^2+\chi_a^2}{2R_a}\right) = \frac{n^2}{2G_a} \quad (5)$$

where $n = 1+(L_1/L_2)$ and $G_a = R_a/(R_a^2+\chi_a^2)$ is the antenna conductance. The imaginary parts of the admittances lead to:

$$L_{eq} = \frac{|Z_a|^2 (L_1+L_2)^2 + 4\omega^2 L_1^2 L_2^2 + 4\omega\chi_a L_1 L_2 (L_1+L_2)}{|Z_a|^2 (L_1+L_2) + 4\omega^2 L_2^2 L_1 + 2\omega\chi_a \left(L_2^2 + 2L_1 L_2\right)} \quad (6)$$

which can be approximated by:

$$L_{eq} = L_1 + L_2 \quad (7)$$

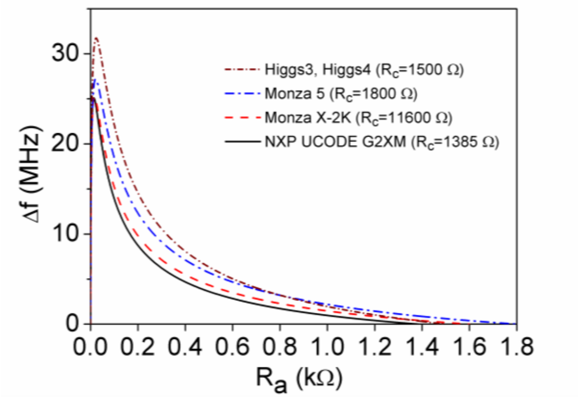

Fig. 6. Frequency increment of the tag resonance (with respect to f_0) as a function of the antenna resistance, R_a, in the case of considering four different commercial chips. Notice that Δf goes to zero when $R_a = R_c$.

provided $(R_a^2+\chi_a^2)(L_1+L_2)^2 >> |4\omega^2L_1^2L_2^2+4\omega\chi_aL_1L_2(L_1+L_2)|$ and $(R_a^2+\chi_a^2)(L_1+L_2) >> |4\omega^2L_2^2L_1+2\omega\chi_a(L_2^2+2L_1L_2)|$ (notice that the first condition is the same than the one required for expression 5). It can be demonstrated through simple algebra that these two inequalities are satisfied if

$$\frac{|Z_a|}{2} \gg |Z_{L_2}| \tag{8}$$

$$|\chi_a| \le |Z_{L_2}| \frac{L_1+L_2}{\max\left\{L_1, \frac{L_2}{2}\right\}} \tag{9}$$

where $|Z_{L2}| = \omega L_2$. Hence, the circuit of Fig. 4 can be approximated by the circuit of Fig. 5, where R_{eq} and L_{eq} are obtained from (5) and (7), respectively, as long as conditions (8) and (9) are satisfied.

III. Design and Synthesis of T-Match based Tags

A systematic methodology for the design and synthesis of a global band T-match based tag is presented in this section. Let us consider the circuit of Fig. 5, assuming that conditions (8) and (9) are well satisfied, as a model for T-match based tags. The central frequency of the operating band is chosen to be the intermediate frequency of the UHF-RFID band, f_0 = 898 MHz. Then, R_{eq} in (5) must be equal to $R_c/2$ and L_{eq} in (7) must be equal to $1/(2\omega_0^2C_c)$, where $\omega_0 = 2\pi f_0$, to achieve complex conjugate matching at f_0. It is clear that, for a given chip and Z_a, the inductances L_1 and L_2 can be easily calculated from (5) and (7). However, in spite of the possibility of satisfying conditions (8) and (9) by means of an antenna with a complex impedance, resonant antennas designed at f_0 are very good candidates for using the proposed circuit approach. This is because, regardless of the considered chip, condition (9) will be easily satisfied in the vicinity of the antenna resonance frequency since χ_a approaches zero. Therefore, the proposed equivalent-circuit model will predict the frequency response of the designed tag in a wider bandwidth when a resonant antenna is considered.

Let us consider the particular case of using a resonant tag antenna designed to exhibit a purely resistive impedance R_a at f_0. It is important to point out that even if conditions (8) and (9) are very well satisfied, a frequency shift of the tag resonance and a reduction of the matching level (with respect to conjugate matching) at this frequency are expected, as long as R_a differs from R_c, since R_{eq} and L_{eq} are exactly determined by (4) and (6) rather than (5) and (7), respectively. However, this frequency shift can be avoided by taking it into account in the T-match design stage, and the matching level at the tag resonance can be predicted. Let us see how this is possible by means of an analysis of the power reflection coefficient of Fig. 5, given by [17], [18]

$$|s|^2 = \left|\frac{Y_{eq}^* - 2Y_{chip}}{Y_{eq} + 2Y_{chip}}\right|^2 = \frac{\left(G_{eq} - 2G_{chip}\right)^2 + B^2}{\left(G_{eq} + 2G_{chip}\right)^2 + B^2} \tag{10}$$

where Y_{chip} is the chip admittance, $G_{chip} = 1/R_c$, $G_{eq}=1/R_{eq}$ and $B = B_{eq}+2B_{chip}$ is the total susceptance of the circuit given by the sum of the susceptance of L_{eq} and two times the susceptance of the chip. Let us assume a constant resistive value for the antenna impedance such that $Z_a = R_a \le R_c$ in the circuit of Fig. 5, where R_{eq} and L_{eq} are given by (4) and (6), respectively. By using (6), it can be demonstrated (see Appendix A) that the susceptance B vanishes at a frequency $\omega \ge \omega_0$, since $L_{eq} \le L_1+L_2 = 1/(2\omega_0^2C_c)$. This corresponds to a frequency shift of the tag resonance, $\Delta\omega = 2\pi\Delta f$, towards higher frequencies, which depends only upon the antenna resistance, for a given chip (see Appendix A). Such shift is depicted in Fig. 6 in the case of considering four different commercial chips [19]-[21]. It can be seen that Δf decreases as R_a approaches the chip resistance, R_c, and becomes higher as R_a moves away (decreasing) from R_c. (The case when $R_a > R_c$ is not necessary to be discussed, since the presented method requires that $R_a \le R_c$). Moreover, a reduction of the matching level (with respect to conjugate matching) will take place at this frequency, as long as R_a differs from R_c. From (4) it follows that the exact expression for G_{eq} evaluated at the tag resonance

$$G_{eq} = \frac{2R_a\omega_0^4C_c^2}{R_aR_c\omega_0^4C_c^2 + \left(\omega_0 + \Delta\omega\right)^2\left(1 - \sqrt{R_a/R_c}\right)^2} \tag{11}$$

is always less than or equal to $2G_{chip}$, and becomes lower as R_a moves away (decreasing) from R_c. Then, by evaluating (10) at the tag resonance ($B = 0$) and introducing (11) into this expression, this matching level reduction can be inferred.

Let us now consider any general complex antenna impedance $Z_a = R_a+j\chi_a$, designed to exhibit a real impedance value at $f_0+\Delta f$ (being Δf the shift related to this real impedance value). Obviously, the same power reflection coefficient as in the previous case (where a constant antenna impedance value was considered) will be achieved at $f_0+\Delta f$, since $B = 0$ and G_{eq} is given by (11) at this frequency. Furthermore, it can be demonstrated from (10) that the minimum power reflection coefficient occurs roughly at that frequency when $B = 0$, even in the case of considering G_{eq} as a frequency dependent function, provided G_{eq} is close to $2G_{chip}$ at that frequency (see Appendix B). Notice that if conditions (8) and (9) are satisfied, R_{eq} is approximately given by (5) and, therefore,

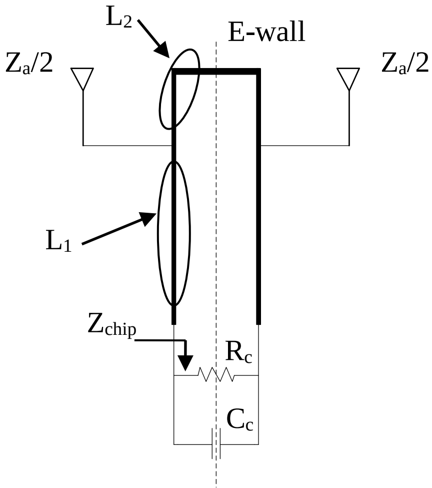

Fig. 7. Model of an UHF-RFID T-match based tag.

$G_{eq} \approx 2G_{chip}$ at the antenna resonance frequency, namely, $f_0+\Delta f$. This can also be seen from equation (11), since G_{eq} approaches $2G_{chip}$ as R_a goes near R_c. Thus, by forcing equation (5) to be $R_c/2$ at the antenna resonance frequency, $f_0+\Delta f$, and $L_{eq} = 1/(2\omega_0^2 C_c)$ in (7), the tag resonance will be located at $f_0+\Delta f$, and the matching level at this frequency can be approximately inferred by introducing (11) into (10) and forcing $B = 0$ and $R_a = Z_a(f_0+\Delta f)$.

A. Design of a T-Match based Tag using a Resonant Antenna

From the above analysis, it can be concluded that the proposed method should be applied by means of a resonant antenna designed at f_0 and the T-match network designed by forcing $R_{eq} = R_c/2$ at f_0 in (5) and $L_{eq} = 1/(2(\omega_0-\Delta\omega)^2 C_c)$ in (7), in order to obtain the tag resonance at the desired frequency, f_0 (notice that a linear approximation of Δf with respect to f_0 has been considered, since $\Delta f << f_0$). The shift Δf is obtained from that curve corresponding to a given chip (see Fig. 6), evaluated at $R_a = Z_a(f_0)$. Then, from (5), the factor n can be rewritten in terms of the chip resistance, R_c, and the antenna resistance evaluated at f_0, $R_a(f_0)$, given $n = 1+(L_1/L_2) = (R_c/R_a(f_0))^{1/2}$. Thus, the inductances L_1 and L_2 can be calculated from (5) and (7) and are obtained as

$$L_1 = \frac{1}{2(\omega_0-\Delta\omega)^2 C_c}\left(1-\frac{1}{n}\right) \tag{12}$$

$$L_2 = \frac{1}{2n(\omega_0-\Delta\omega)^2 C_c} \tag{13}$$

Then, the required conditions (8) and (9) lead to

$$|Z_a| \gg \frac{1}{n\omega_0 C_c} \tag{14}$$

$$|\chi_a| \le \begin{cases} \dfrac{1}{\omega_0 C_c} & \text{if} \quad 1 \le n \le \dfrac{3}{2} \\ \dfrac{1}{2\omega_0 C_c (n-1)} & \text{if} \quad n > \dfrac{3}{2} \end{cases} \tag{15}$$

where, it has been considered $\omega \approx \omega_0$ and $(\omega_0-\Delta\omega) \approx \omega_0$, since variations of ω relative to ω_0 are less than 7 % within the whole UHF-RFID band and $\Delta\omega << \omega_0$. Notice that condition (15) does not play any role to achieve complex conjugate matching at f_0, since $\chi_a = 0$ at this frequency (this condition will be used in section III(c) to discuss the frequency range of validity of the proposed circuit approach). However, expression (14) lead to a simple condition, in which the required antenna resistance $R_a(f_0)$ depends only upon the RFID chip and the intermediate frequency as $R_a(f_0) >> 1/(\omega_0^2 C_c^2 R_c)$. Therefore, the greater the value of $R_a(f_0)$, the better satisfied the required condition. However, since R_{eq} is forced to be $R_c/2$ at f_0, as indicated before, it follows from (5) that $R_a(f_0)$ must be less than or equal to R_c. Hence, it can be concluded that the presented approach is valid at the intermediate frequency, if the antenna resistance accomplishes

$$\frac{1}{\omega_0^2 C_c^2 R_c} \ll R_a(f_0) \le R_c \tag{16}$$

Notice that condition (16) forces $(R_c C_c)^2 >> 1/\omega_0^2$, which is well satisfied by the typical values of the RFID integrated circuits available on the market today, such as Impinj Monza 5, Impinj Monza X-2K Dura, Alien Higgs 3, Alien Higgs 4 and NXP UCODE G2XM [19]-[21].

B. Tag Bandwidth Related to the Antenna Impedance

Let us now demonstrate that a degradation of the maximum achievable tag bandwidth, by means of the proposed equivalent-circuit approach and considering conjugate matching at f_0, will be mainly determined by the derivative of the antenna resistance at f_0. It was demonstrated in [22] that the optimum equivalent-circuit network necessary for bandwidth broadening in single resonant UHF-RFID tags with conjugate matching is a parallel combination of an inductor and a resistor cascaded to the chip, according to the Bode's limit [23], [24]. However, the proposed circuit approach consists of a parallel combination of an inductor and a frequency dependent resistor, cascaded to the chip. Hence, bandwidth degradation with respect to the optimum will be obtained as long as the conductance G_{eq} differs from $2G_{chip}$. In a first order approximation, this reduction of the tag bandwidth is determined by the frequency derivative of the antenna resistance at f_0, and it does not depend on the frequency derivative of the antenna reactance χ_a, since this term is cancelled. This result is deduced from the first-order Taylor expansion of the conductance G_{eq}, obtained from (5), in the vicinity of f_0

$$G_{eq} = 2G_{chip}\left(1-\frac{R_a'(f_0)}{R_a(f_0)}(f-f_0)\right) \tag{17}$$

where $R_a'(f_0)$ is the frequency derivative of the antenna resistance evaluated at f_0. Notice that, for a given value of $R_a(f_0)$, the further $R_a'(f_0)$ is from zero, the further G_{eq} is from $2G_{chip}$, and consequently a higher degradation of the tag bandwidth will be obtained. By introducing (17) into (10) and expanding the susceptance $B = B_{eq}+2B_{chip}$ (using $L_{eq} = 1/(2\omega_0^2 C_c)$, the approximated bandwidth at a fixed value

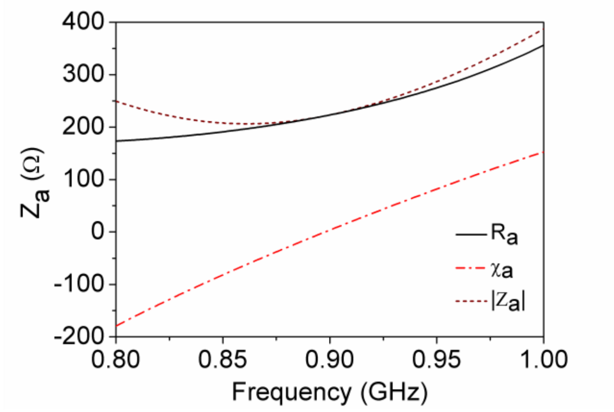

Fig. 8. Input impedance of the designed tag antenna.

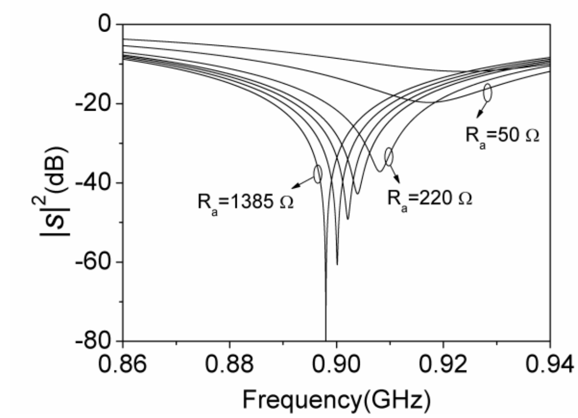

Fig. 9. Simulated power reflection coefficient of the circuit of Fig. 4, by sweeping the antenna impedance Z_a from 20 Ω to 1385 Ω.

for the power reflection coefficient can be inferred, within the frequency range of validity of the proposed circuit approach.

C. Frequency Range of Validity of the Proposed Approach

Let us now focus on the validity of the presented approach beyond the tag resonance frequency. As it has been pointed out, a T-match based tag designed following the steps indicated in Section III(a) will exhibit a frequency response centered at the desired frequency f_0. Therefore, such a response will be similar to that of the proposed equivalent-circuit of Fig.5, using (5) and (7) and designing the T-match network at f_0. It follows that, in order to determine the frequency range of validity of the proposed approach, a comparison between these two frequency responses makes sense. Then, assuming that the tag antenna satisfies the required condition at the resonance frequency (see expression 16), an examination of condition (14) reveals that it will be satisfied within the whole UHF-RFID band provided $|Z_a| \geq R_a(f_0)$. It can be easily demonstrated that this condition holds true in the case of considering a canonic *RLC* series load as antenna impedance. Thus, in this particular case, condition (14) is accomplished in all frequencies and, consequently, the frequency limits around the tag resonance from which the proposed approach no longer predicts the frequency response of the designed tag are determined by (15). Therefore, in order to satisfy such condition within the entire UHF-RFID band, the frequency derivative of χ_a must be small. Conversely, if the antenna impedance can be approximated by an *RLC* shunt load around the resonance frequency, both expressions (14) and (15) must be taken into account in order to obtain the frequency limits from which the proposed approach becomes invalid. This is exactly what happens by considering any general frequency dependent complex antenna impedance. Thus, in such cases, both the frequency derivatives of χ_a and R_a should be small to enhance the frequency range of validity.

D. Synthesis of a T-Match based Tag using a Resonant Antenna

A simple method for the synthesis of T-match based tags using a resonant antenna is proposed in this section. In order to synthesize the T-match network, we start by considering a closed loop consisting of a narrow conductor strip (e.g. 0.2 mm width) connected to a differential port with impedance Z_{chip}, as depicted in Fig. 7. This loop exhibits an inductive behavior at the UHF-RFID frequency band. To achieve the required dimensions for the loop inductance, a sweep of the length of the loop is carried out by means of electromagnetic simulations (by using the *Agilent Momentum* commercial software), until the resonance frequency appears at $f_0 – \Delta f$. Then, the inductance corresponding to one half of the loop must be divided into L_1 and L_2 by connecting the antenna at the adequate position (see Fig. 7). To this end, a sweep of the position of the antenna connection is carried out to achieve the calculated values for these inductances. The final position is obtained when the tag resonance reaches the desired frequency f_0.

IV. Design of a Broadband UHF-RFID Tag using the Proposed Method

Let us now consider a typical integrated circuit for the RFID tag (the NXP UCODE G2XM chip). The impedance reported by the manufacturer of this integrated circuit is $Z_{chip} = 16 – j148$ Ω, at 915 MHz. As indicated in Section II, the chip can be modeled by a parallel combination of a resistance R_c and a capacitance C_c. These values were calculated from the input impedance of the chip transformed to its equivalent *RC* parallel circuit, giving $R_c = 1385$ Ω and $C_c = 1.16$ pF. From (16) it follows that $17\ \Omega << R_a(f_0) \leq 1385\ \Omega$. Thus, the tag antenna has to be designed to exhibit an antenna resistance at the operating frequency according to (16). As a proof of concept for the presented method, an antenna for tag implementation was designed on a commercial low loss microwave substrate, the *Rogers RO3010* substrate with dielectric constant $\varepsilon_r = 10.2$ and thickness $h = 0.254$ mm. As it was pointed out, the use of a resonant antenna becomes appropriate to ensure the validity of the presented approach around the operating frequency f_0. The proposed antenna is a meandered coplanar strip, folded dipole working at the so called antenna mode [25]-[28], which allows the antenna impedance (at least the imaginary part) to be approximated by the canonic *RLC* series load, around the antenna resonance frequency f_0. The designed antenna exhibits a purely resistive impedance at the intermediate frequency, $R_a(f_0) = 220$ Ω (see

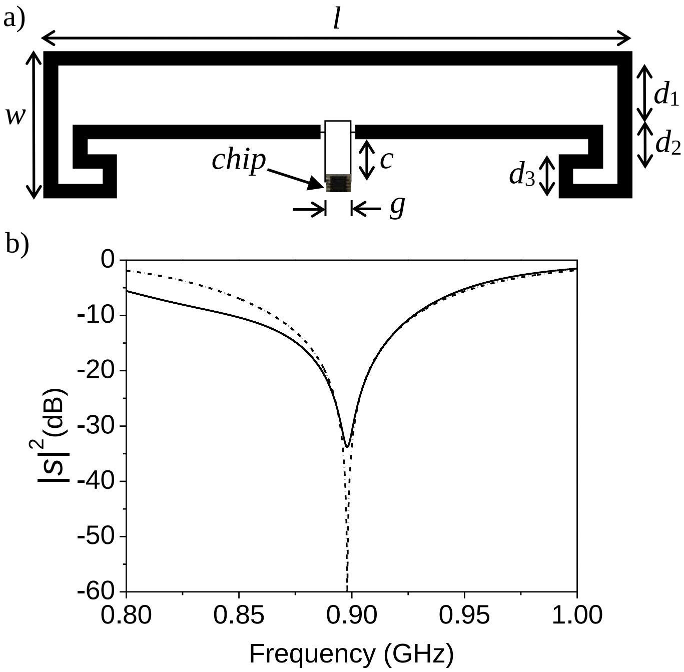

Fig. 10. (a) Layout of the designed T-match based tag. (b) Electrical simulation of the return loss of the proposed equivalent-circuit (dash dot line) and electromagnetic simulation of the return loss of the designed tag (solid line).

Fig. 8). Then, in order to design the T-match network at the correct frequency f_0–Δf, the frequency shift was inferred by using expression (A4) and it was found to be 8 MHz. This result perfectly agrees with the shift obtained in Fig. 9, where a simulation (by means of the *Agilent ADS* circuit simulator) of the power reflection coefficient of the circuit of Fig.5, using (5) and (7) and designing the T-match network at f_0, with a sweep of the antenna impedance $Z_a = R_a$ from 20 Ω to 1385 Ω, is depicted. As expected in this analysis, perfect conjugate matching at the desired frequency f_0 is achieved when $R_a = R_c$ and, consequently, $L_1 = 0$ and $L_2 = 1/(2\omega_0^2 C_c)$. This is because in this case, approximation (7) becomes an exact expression for L_{eq} and $G_{\text{eq}} = 2G_{\text{chip}}$. As it was previously predicted, a frequency shift of the tag resonance from f_0 toward higher frequencies and a reduction of the matching level at this frequency are observed as R_a decreases from R_c. It can be seen in Fig. 9 that such frequency shift and matching level reduction at the resonance frequency become more significant as the value of R_a moves away from R_c. Thus, the T-match network was designed at 890 MHz, which corresponds to 8 MHz below f_0. From (12) and (13), the elements of the T-match network where found to be $L_1 = 8.3$ nH and $L_2 = 5.5$ nH. Then, the synthesis method explained in the previous section was applied. The layout of the designed tag is depicted in Fig. 10(a). The dimensions are l=120 mm, w=30 mm, g=4.9 mm, c=8.7 mm, d_1=12 mm, d_2=9 mm and d_3=9 mm. All the strips of the antenna have the same width (3 mm) and the width of the T-match network is 0.2 mm. The total length of the T-match closed loop was found to be 30 mm, and the tag antenna was connected to the loop at a distance of 10.2 mm from the chip. The power reflection coefficient of the designed RFID tag is depicted in Fig. 10(b).

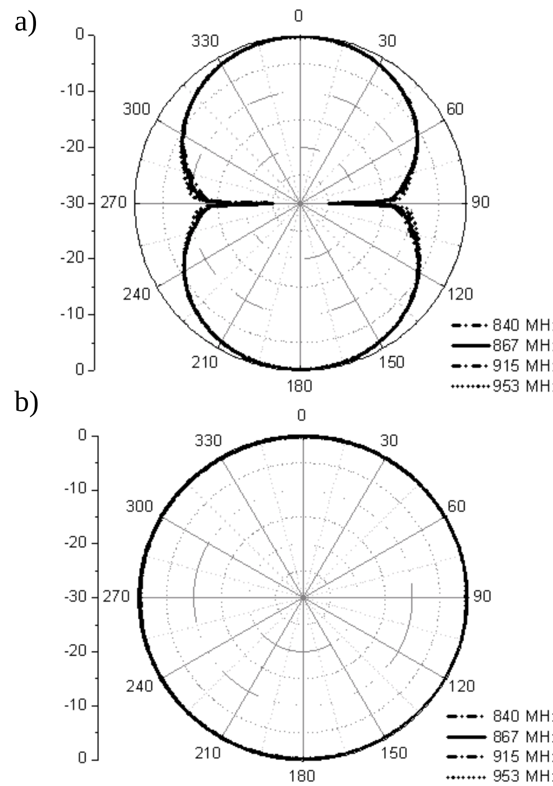

Fig. 11. (a) Electric plane radiation pattern of the designed T-match based tag and (b) magnetic plane. The proposed tag has a radiation pattern similar to that of a conventional λ/2 dipole in the whole UHF-RFID band.

It can be seen that conjugate matching is achieved at the intermediate frequency f_0 of the UHF-RFID frequency band. Very good agreement is observed between the power reflection coefficient obtained from the equivalent-circuit approach and the electromagnetic simulation within the entire UHF-RFID band except in the low frequency region. Although the tag antenna exhibits purely resistive impedance at the resonance frequency f_0, the antenna resistance is not constant with frequency, as it is shown in Fig. 8. Hence, both conditions (14) and (15) must be examined to discuss the validity of the approach applied in this work within the UHF-RFID band, as it was mentioned in Section III(c). For the considered chip and antenna impedance, we obtain $|Z_a| >> 61\ \Omega$ and $|\chi_a| \leq 51\ \Omega$. Thus, the condition for the antenna reactance is satisfied between 867 MHz and 930 MHz. However, although the condition for the absolute value of the antenna impedance is well satisfied at frequencies higher than f_0 and in the vicinity, there is a frequency region within the low UHF-RFID band where such condition is less satisfied. Therefore, good agreement is expected between the power reflection coefficients of the equivalent-circuit approach and the electromagnetic response of the designed tag within the whole UHF-RFID band, except in the low frequency region.

As indicated in Section III(b), by introducing (17) into (10), the approximated bandwidth at a fixed value for the power reflection coefficient can be predicted, within the frequency range of validity of the proposed circuit approach. Thus, the –15 dB bandwidth was found to be 35 MHz, which is similar

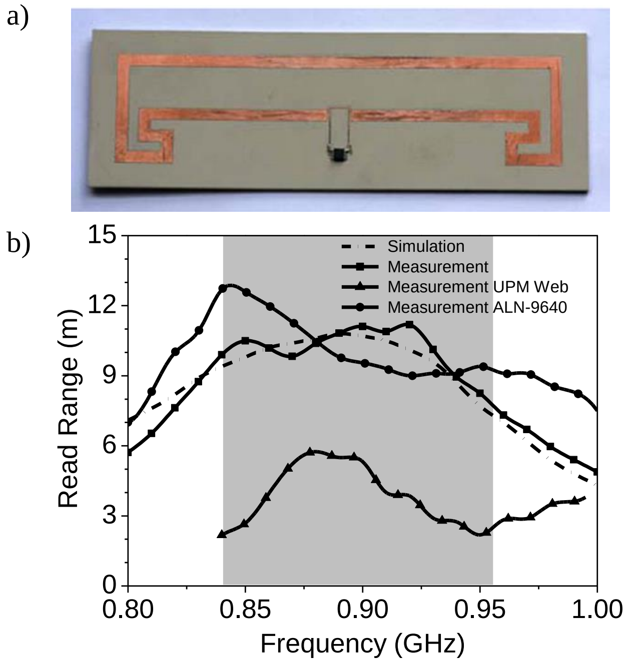

Fig. 12. (a) Photograph of the fabricated RFID tag and (b) simulated and measured read range. The measured read ranges of the *UPM Web* tag (that uses the tag chip of our prototype), and the *Alien ALN-9640* tag of Fig. 1, are also shown for comparison purposes.

to the obtained by means of the electromagnetic simulation of the designed tag (39 MHz). The simulated gain reaches the value of 1.8 dBi at the operating frequency and the radiation pattern is similar to that of a conventional λ/2 dipole in the whole UHF-RFID band, as it is shown in Fig. 11.

V. Fabrication and Measurement

A. Theoretical Read Range

To determine the performance of the tags, it is necessary to obtain the read range [29], which can be calculated using the Friis free space formula as

$$r = \frac{\lambda}{4\pi}\sqrt{\frac{EIRP\ G_r \tau}{P_{chip}}} \qquad (18)$$

where λ is the wavelength and *EIRP* is the equivalent isotropically radiated power, determined by local country regulations (e.g. 3.3W in Europe and 4W in USA). P_{chip} is the minimum threshold power necessary to activate the RFID chip, G_r is the gain of the receiving tag antenna, and τ is the power transmission coefficient, which is related to the power reflection coefficient $|s|^2$ by $\tau = (1-|s|^2)$. The tag gain and the power transmission coefficient are inferred from simulation, using as port impedance that of the chip. Despite the minimum power level necessary to activate the chip used in this work reported by the manufacturer is $P_{\text{chip}} = -15$ dBm, a different threshold power was obtained in [30]. In such work it was found that P_{chip} exhibits a lower and frequency dependent value. Taken it into account and from electromagnetic and circuit co-simulation results, an evaluation of the theoretical read range was obtained and depicted in Fig. 12(b).

B. Measured Read Range and Experimental Setup

The RFID setup available in our laboratory has an *Agilent N5182A* vector signal generator, which creates RFID frames and plays the role of a reader with variable frequency and variable output power. Such generator is connected to a TEM cell by means of a circulator. The tag under test is located inside the TEM cell and it is excited by the frame created by the generator. Then the tag sends a backscatter signal to an *Agilent N9020A* signal analyzer through the circulator. At each frequency, the minimum power at the input of the TEM cell required to communicate with the tag is recorded. Finally, an electric probe is placed into the TEM cell to determine the root mean square of the incident electric field, E_{rms}, corresponding to the minimum power at each frequency. This electric field is related to the power delivered to the chip according to

$$P_{chip} = SA_{ef}\tau = \frac{|E_{rms}|^2}{\eta}\frac{\lambda^2 G_r}{4\pi}\tau \qquad (19)$$

where S is the incident power density, A_{ef} is the effective area of the tag antenna, and η is the wave impedance of free space. The measured read range can be inferred by introducing (19) into (18), resulting the following expression

$$r = \frac{\sqrt{30 EIRP}}{E_{rms}} \qquad (20)$$

C. Experimental Results

The proposed RFID tag was fabricated and the read range was measured (see Fig. 12) through the procedure explained above. Very good agreement between the theoretical and measured read ranges can be observed. The fabricated tag exhibits a significant read range within the whole UHF-RFID band (840-960 MHz), with a peak value of 11 m at 898 MHz. The read range of a commercially available tag (*UPM Web*) that uses the *NXP UCODE G2XM* chip and the T-match network is also shown in Fig. 12(b) for comparison purposes. It can be seen that our fabricated tag exhibits a substantially superior read range in the whole UHF-RFID band. Despite the fact that comparing RFID tags only makes sense if they use the same chip (the chip impedance and P_{chip} are key parameters in determining the read range), we have also included in Fig. 12(b) the read range of the commercial tag *Alien ALN-9640* (Fig. 1). Such tag uses a chip (the *Alien Higgs 3*) with $P_{\text{chip}} = -18$ dBm, whereas $P_{\text{chip}} = -15$ dBm for the *NXP UCODE G2XM* chip (according to the manufacturer specifications). In spite of this significant difference in the threshold power, the read range at 898 MHz is comparable in both the *ALN-9640* tag and our proposed tag. Therefore, the proposed approach for the design of global band UHF-RFID tags is simple and competitive in terms of the main figure of merit: the read range.

VI. Conclusion

In this paper, a systematic and simple method for the design of UHF-RFID tags, based on the T-match network, has been introduced. This method is based on a new equivalent-circuit model for the RFID tag that includes the tag antenna, the chip and the matching network. The main advantage provided by this method, in comparison with the methods reported in the literature, relies in the ease to synthesize the T-match network required to achieve a broad band frequency response, with conjugate matching between the chip and the antenna at a certain frequency. Even though, such antenna must be previously designed to exhibit a self-resonance at f_0. As a proof of concept, a global band tag has been designed using this method, and the read range of the fabricated prototype has been measured and compared to those of commercially available tags. The results reveal that the designed tag is very competitive, and point out that the proposed circuit-based approach is very useful for the synthesis of T-match based tags.

Appendix

A. Calculation of the Frequency shift of the Tag Resonance

Let us consider the circuit of Fig. 4, where the tag antenna has a purely resistive impedance such that $Z_a = R_a \le R_c$. This circuit can be exactly modeled by the one depicted in Fig. 5, where R_{eq} and L_{eq} are given by (4) and (6), respectively. Now, if we use equations (5) and (7) in the circuit of Fig. 5 rather than (4) and (6), one can obtain the inductances L_1 and L_2

$$L_1 = \frac{1}{2\omega_0^2 C_c}\left(1 - \frac{1}{n}\right) \quad \text{(A1)}$$

$$L_2 = \frac{1}{2n\omega_0^2 C_c} \quad \text{(A2)}$$

It follows that the exact expression for the inductance L_{eq} in the circuit of Fig. 5 can be expressed as

$$L_{eq} = (L_1 + L_2)\left[\frac{4\omega^2 (L_1 + L_2)^2 \left(1 - \frac{1}{n}\right)^2 + R_a R_c}{4\omega^2 (L_1 + L_2)^2 \left(1 - \frac{1}{n}\right) + R_a R_c}\right] \quad \text{(A3)}$$

where $n \ge 1$. Hence, it is clear from (A3) that $L_{eq} \le L_1 + L_2$ and, therefore, the susceptance $B = B_{eq} + 2B_{chip}$ vanishes at a frequency $\omega \ge \omega_0$. This frequency can be inferred by forcing $B = 0$ and using (A3), giving a frequency increment, $\Delta\omega$, of the tag resonant with respect to ω_0 which can be written as (see A4).

B. Minimum Power Reflection Coefficient

Let us now consider the circuit depicted in Fig. 4, where the tag antenna has any general complex impedance $Z_a = R_a + j\chi_a$ and χ_a being an arbitrary frequency dependent function. This circuit can be exactly modeled by the one depicted in Fig. 5, where R_{eq} and L_{eq} are given by (4) and (6), respectively. Then, $G_{eq} = 1/R_{eq}$ also results in an arbitrary frequency dependent function. Let us demonstrate that in the case when $G_{eq} \approx 2G_{chip}$, the minimum power reflection coefficient occurs roughly at that frequency when the total susceptance $B = B_{eq} + 2B_{chip}$ vanishes. The power reflection coefficient, $|s|^2$, from the circuit of Fig. 5 is given by expression (10). By forcing the frequency derivative of (10) to be zero, it is found that

$$2BB'G_{eq} = G'_{eq}\left(B^2 + 4G_{chip}^2 - G_{eq}^2\right) \quad \text{(B1)}$$

where B' and G'_{eq} are the frequency derivatives of the susceptance B and the conductance G_{eq}, respectively. Notice that all the parameters in (B1) are frequency dependent functions, except G_{chip}. It can be deduced that equation (B1) is satisfied at that frequency when $B = 0$, provided that $G_{eq} = 2G_{chip}$.

References

[1] K. Finkenzeller, *RFID Handbook: Radio-Frequency Identification Fundamentals and Applications*, 2nd ed: Wiley, 2004.

[2] G. Marrocco, "The art of UHF-RFID antenna design: impedance matching and size-reduction techniques," *IEEE Antennas and Propagation Magazine*, vol. 50, no. 1, pp. 66–79, Feb. 2008.

[3] F. Paredes, G. Zamora, J. Bonache, and F. Martin, "Dual-band impedance-matching networks based on split-ring resonators for applications in RF identification (RFID)", *IEEE Transactions on Microwave Theory and Techniques*, vol. 58, no. 4, pp. 1159–1166, April 2010.

[4] J. Choo, J. Ryoo, J. Hong, H. Jeon, C. Choi and M. M. Tentzeris, "T-matching networks for the efficient matching of practical RFID tags", *European Microwave Conference*, pp. 5–8, 2009.

[5] D. D. Deavours, "Analysis and design of wideband passive UHF-RFID tags using a circuit model", *IEEE International Conference on RFID*, 283–290, May 2009.

[6] N. A. Mohamed, K. R. Demarest and D. D. Deavours, "Analysis and synthesis of UHF RFID antennas using the embedded T-match", *IEEE International Conference on RFID*, pp. 230–236, April 2010.

[7] S. Uda and Y. Mushiake, *Yagi-Uda Antenna*. Tohoku University: Research Institute of Electrical Communication, 1954.

[8] C. A. Balanis, *Antenna Theory: Analysis and Design*, 3rd ed., John Wiley & Sons Inc., NY, 2005.

[9] R. W. Lampe, "Design formulas for an asymmetric coplanar strip folded dipole', *IEEE Trans. Antennas Propagation*, vol. AP–33, no. 9, pp. 1028–1031, 1985.

[10] W. Lampe, Correction to "Design formulas for an asymmetric coplanar strip folded dipole', *IEEE Trans. Antennas Propagation*, vol. AP-34, no. 4, pp. 611, 1986.

[11] H. J. Visser, "Improved design equation for asymmetric coplanar strip folded dipoles on a dielectric slab," *Antennas and Propagation International Symposium*, pp. 1–6, 2007.

[12] D. M. Dobkin and S. Weigand, "Environmental effects on RFID tag antennas," IEEE MTT–S International Microwave Symposium, pp. 135–138, June 2005.

[13] D. M. Dobkin, *The RF in RFID: Passive UHF RFID in Practice*, Newnes, 2007.

[14] E. Bergeret, J. Gaubert, P. Pannier and J.M. Gaultier, "Modeling and design of CMOS UHF voltage multiplier for RFID in a EEPROM compatible process" *IEEE Trans. Circuits and Systems*, vol. 54, pp.833-837, Oct. 2007.

[15] G. De Vita and G. Iannaccome, "Design Criteria for the RF section of UHF and microwave passive RFID transponders", *IEEE Trans. Microwave Theory Tech*., vol. 53, no. 9, pp. 2978–2990, Sep. 2005.

[16] P. H. Young, *Electronic Communication Techniques*, 3rd ed., Macmillan Publishing Company, NY, 1994.

$$\Delta\omega = \sqrt{\frac{\omega_0^2 C_c\left(1 - \sqrt{R_a/R_c}\right) - \omega_0^4 C_c^3 R_a R_c + \sqrt{\left[\omega_0^2 C_c\left(1 - \sqrt{R_a/R_c}\right) - \omega_0^4 C_c^3 R_a R_c\right]^2 + 4\omega_0^6 C_c^4 R_a R_c \left(1 - \sqrt{R_a/R_c}\right)^2}}{2C_c\left(1 - \sqrt{R_a/R_c}\right)^2}} - \omega_0 \quad \text{(A4)}$$

[17] K. Kurokawa, "Power waves and the scattering matrix", *IEEE Trans. Microw. Theory Tech*., vol. MTT-13, no. 3, pp. 194–202, Mar. 1965.
[18] P. V. Nikitin, K. V. Seshagiri Rao, S. F. Lam, V. Pillai, R. Martinez, and H. Heinrich, "Power Reflection Coefficient Analysis for Complex Impedances in RFID Tag Design", *IEEE Trans. Antennas and Propagation*, vol. 53, pp. 2721–2725, Sep. 2005.
[19] Impinj RFID chips [Online]. Available: http://www.impinj.com
[20] Alien Technology RFID Ics [Online]. Available : http://www.alientechnology.com
[21] NXP UCODE smart label ICs [Online]. Available: www.nxp.com
[22] G. Zamora, F. Paredes, F. J. Herraiz-Martinez, and F. Martin and J. Bonache "On the bandwidth limitations of UHF-RFID tags", *IET Microwaves Antennas and Propagation.* Accepted (May 2013).
[23] H. W. Bode, "Network analysis and feedback amplifier design", pp. 360–371, D. Van Nostrand co., N.Y., 1945.
[24] R. M. Fano, "Theoretical Limitations on the Broadband Matching of Arbitrary Impedances," Journal of the Frank1in Institute, vol. 249, pp. 57–154, 1950.
[25] W. L. Weeks, *Antenna Engineering*. McGraw-Hill, NY, 1968.
[26] H. Jasik, Ed., *Antenna Engineering Handbook*, McGraw-Hill, NY, 1961.
[27] G. A. Thiele, E. P. Ekelman, and L. W. Henderson, "On the accuracy of the transmission line model of the folded dipole," *IEEE Trans. Antennas Propagation*, vol. AP-28, pp. 700–703, Sep., 1980.
[28] A. R. Clark and A. P. C Fourie, "An improvement to the transmission line model of folded dipole," *IEE Proc Microwave Antennas Propag*, Vol. 138, no. 6, 577–579, Dec. 1991.
[29] K. V. Seshagiri Rao, P. V. Nikitin, and S. F. Lam, "Antenna design for UHF-RFID tags: a review and a practical application", *IEEE Trans. Antennas and Propagation*, vol. 53, pp. 3870–3876, Dec. 2005.
[30] P. V. Nikitin, K. V. Seshagiri Rao, R. Martinez, S. F. Lam, "Sensitivity and impedance measurements of UHF-RFID chips," *IEEE Trans. Microw. Theory Tech.*, vol. 57,no. 5, pp. 1297–1302, May 2009.

Gerard Zamora Gonzalez was born in 1984 in Barcelona (Spain). He received the Telecommunications Engineering Diploma, specializing in Electronics from the Universitat Autònoma de Barcelona in 2005. He obtained the Telecommunications Engineering degree in 2008. He is currently working toward his PhD degree at the Universitat Autònoma de Barcelona. His research interests include passive microwave devices based on metamaterial concepts and antenna design for RFID systems.

Simone Zuffanelli was born in Prato (Italy) in 1983. He received the Electronics Engineering Diploma in 2008 at the Università Degli Studi di Firenze. He obtained "Micro and Nanoelectronics Engineering" master's degree in 2011 at the Universitat Autònoma de Barcelona. He is currently working as a researcher in the field of metamaterial inspired antennas and RFID tags. His previous experiences include electronic design in the context of European projects "Persona" and "NOMS".

Ferran Paredes was born in Badalona (Barcelona), Spain in 1983. He received the Telecommunications Engineering Diploma (specializing in Electronics) and the Telecommunications Engineering degree from the Universitat Autònoma de Barcelona in 2004 and 2006, respectively and the PhD degree in Electronics Engineering from the same university in 2012. He was Assistant Professor from 2006 to 2008 at the Universitat Autònoma de Barcelona, where he is currently working as a Research Assistant. His research interests include metamaterial concepts, passive microwaves devices, antennas and RFID.

Ferran Martín (M'04-SM'08-F'12) was born in Barakaldo (Vizcaya), Spain in 1965. He received the B.S. Degree in Physics from the Universitat Autònoma de Barcelona (UAB) in 1988 and the PhD degree in 1992. From 1994 up to 2006 he has been Associate Professor in Electronics at the Departament d'Enginyeria Electrònica (Universitat Autònoma de Barcelona), and from 2007 he is Full Professor of Electronics. In recent years, he has been involved in different research activities including modelling and simulation of electron devices for high frequency applications, millimeter wave and THz generation systems, and the application of electromagnetic bandgaps to microwave and millimeter wave circuits. He is now very active in the field of metamaterials and their application to the miniaturization and optimization of microwave circuits and antennas. He is the head of the Microwave and Millimeter Wave Engineering Group (GEMMA Group) at UAB, and director of CIMITEC, a research Center on Metamaterials supported by TECNIO (Generalitat de Catalunya). He has organized several international events related to metamaterials, including Workshops at the IEEE International Microwave Symposium (years 2005 and 2007) and European Microwave Conference (2009). He has acted as Guest Editor for three Special Issues on Metamaterials in three International Journals. He has authored and co-authored over 350 technical conference, letter and journal papers and he is co-author of the monograph on Metamaterials entitled Metamaterials with Negative Parameters: Theory, Design and Microwave Applications (John Wiley & Sons Inc.). Ferran Martín has filed several patents on metamaterials and has headed several Development Contracts. Among his distinctions, Ferran Martín has received the 2006 Duran Farell Prize for Technological Research, he holds the Parc de Recerca UAB – Santander Technology Transfer Chair, and he has been the recipient of an ICREA ACADEMIA Award.

Jordi Bonache (S'05-M'07) was born in 1976 in Barcelona (Spain). He received the Physics and Electronics Engineering Degrees from the Universitat Autònoma de Barcelona in 1999 and 2001, respectively and the PhD degree in Electronics Engineering from the same university in 2007. In 2000, he joined the "High Energy Physics Institute" of Barcelona (IFAE), where he was involved in the design and implementation of the control and monitoring system of the MAGIC telescope. In 2001, he joined the Department of Electronics Engineering of the Universitat Autònoma de Barcelona where he is currently Lecturer. From 2006 to 2009 he worked as executive manager of CIMITEC. Currently he is leading the research in RFID and antennas in CIMITEC. His research interests include active and passive microwave devices, metamaterials, antennas and RFID.